Role of tensile stress in actin gels and a symmetry-breaking instability

K. Sekimoto[a], J. Prost[b], F. Jülicher[c], H. Boukellal, and A. Bernheim-Grosswasser[d]

Physico-Chimie, UMR168 Institut Curie, 26 rue d'Ulm, 75248 Paris Cedex 05, France

Abstract. It has been observed experimentally that the actin gel grown from spherical beads coated with polymerization enzymes spontaneously breaks the symmetry of its spherical shape, and yields a "comet" pushing the bead forward. We propose a mechano-chemical coupling mechanism for the initialization of this symmetry breaking. Key assumptions are that the dissociation of the gel takes place mostly in the region of the external surface, and that the rates of the dissociation depend on the tensile stress in the gel. We analyze a simplified two-dimensional model with a circular substrate. Our analysis shows that the symmetric steady state is always unstable against the inhomogeneous modulation of the thickness of the gel layer, for any radius of the circular substrate. We argue that this model represents the essential feature of three-dimensional systems for a certain range of characteristic lengths of the modulation. The characteristic time of the symmetry-breaking process in our model depends linearly on the radius of curvature of the substrate surface, which is consistent with experimental results, using spherical latex beads as substrate. Our analysis of the symmetry-breaking phenomenon demonstrates aspects of mechano-chemical couplings that should be working *in vivo* as well as *in vitro*.

PACS. 87.17.Jj Cell locomotion; chemotaxis and related directed motion – 87.15.Rn Reactions and kinetics; polymerization – 62.40.+i Anelasticity, internal friction, stress relaxation, and mechanical resonances

1 Introduction

Polymerization of actin is one of the main mechanisms responsible for cellular motility. Filaments of F-actin are polymerized on the cytoplasmic side of a cellular membrane with the barbed ends oriented towards the surface of the membrane. The branching of the actin filaments takes place mainly in the vicinity of the surface. The resulting branched F-actin filaments take the form of a soft elastic solid [1], which we call an actin gel or a gel, simply. This actin gel pushes the cellular membrane outwards. Polymerization of actin gels is also a locomotive mechanism for intracellular bacteria like *Listeria monocytogenes*, and perhaps also for the endosomes and lysosomes [2]. In these cases, the gel is grown in form of a comet. This

comet pushes the bacterium forward. For the purpose of understanding this mechanism of motility, various experimental model systems have been developed using both biochemical and biophysical approaches.

Biochemical approaches have isolated the basic cytoplasmic ingredients needed for the motility of *Listeria monocytogenes* [3]: 1) actin and ATP for the formation of F-actin filaments; 2) Arp2/3 as the cross-linker and/or the nucleator of the F-actin growth (*i.e.*, the precise role is still under debate); 3) ADF as the depolymerization factor at the pointed end of F-actin; 4) the capping protein; 5) a bacterial protein called ActA expressed on the surface of *Listeria* which is necessary for inducing polymerization from the surface. These ingredients constitute a model cytoplasm for the motility.

Biophysical approaches have taken the *Listeria* as a model system of cellular motility. Furthermore, a biomimetic *in vitro* system of the bacterial motility has been introduced. This system consists of a spherical latex bead, coated by the enzymatic protein complexes, ActA [4,5], or a fragment (called the VCA domain) of its homologue from human cells, WASP (Wiskott-Aldrich-Syndrome Protein) [6,7]. The cytoplasm has also been replaced by the reconstituted cytoplasm [7]. Despite the

---

[a] *Present address*: Université Louis Pasteur, 3 rue de l'Université, 67084 Strasbourg, France; e-mail: `sekimoto@ldfc.u-strasbg.fr`.
[b] Also at ESPCI, 10 rue Vauquelin, 75231 Paris Cedex 05, France.
[c] *Present address*: Max Planck Institut für Physik komplexer Systeme, Nöthnitzer Str. 38, 01187 Dresden, Germany.
[d] *Present address*: Chemical Engineering Department, Ben-Gurion University, P.O. Box 653, 84105 Beer-Sheva, Israel.
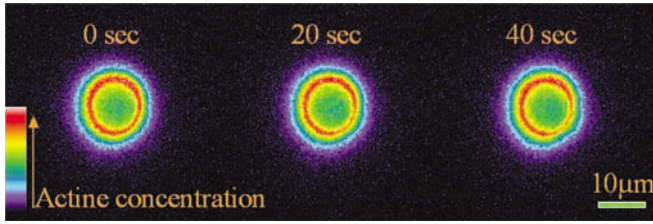
Fig. 1. Experimentally observed time sequence of the actin gel grown around a spherical latex bead. The diameter of the bead is 10 μm. The bead is coated with a fragment of WASP, and it is placed in a reconstituted solvent as described in the text. The actin monomers in the gel is visible by a fluorescent marker. The observation started at $t = 0$ after several tens of seconds when gel has started to grow.

spherical form of the bead, the gel has grown in shape of a comet, like the bacteria *Listeria* (see for example Fig. 2 of [6]). Figure 1 shows the initial stage of the creation of the comet, observed using fluorescent probe attached to actin monomers. This process bares the signature of a spontaneous symmetry breaking, which is the subject of the present paper. The phenomenon of the symmetry breaking is relevant to some biological systems of sub-cellular level. For instance, the endosomes, which consist of spherical soft substrates (liquid vesicles), grow a comet [2]. Also, the motility of a mutant *Listeria*, which moves preferentially in lateral directions [8] grows the actin gel by breaking its cylindrical symmetry. Our principal aim is to assess, through the study of the symmetry breaking, the relevance of the elastic aspects to the biological motilities based on the polymerization of protein filaments, and to provide for several basic ingredients related to the mechano-chemical coupling. The three ingredients essential for explaining the symmetry breaking are (details will be given in Sects. 2–4):

i) *The creation of a tensile stress due to the curvature of the substrate surface* (Sect. 2).
   As the gel is continuously created at the bead surface (at radius, $r = r_0$), the part that has been already formed is continuously pushed outwards ($r > r_0$). Since the perimeter ($2\pi r$) increases as r, and since the surface has a closed topology, the gel is stretched by the ratio, $r/r_0 (> 1)$.

ii) *The concentration of the tensile stress by a geometrical effect* (Sect. 3).
   The gel layer around a bead is in mechanical equilibrium, so that the integrated tension across the layer thickness of the gel must be constant along the surface of the bead. In particular, if the thickness is locally thinner, such a region must bear a stronger tension in order to support the same integrated tension.

iii) *The acceleration of dissociation of the gel under tensile stress* (Sect. 4).
   We suppose that, under tensile stress, the gel dissociation is accelerated through the mechano-chemical coupling. This dissociation may be either through the unbinding of the branching points along actin filaments, or through the depolymerization of actin filaments.
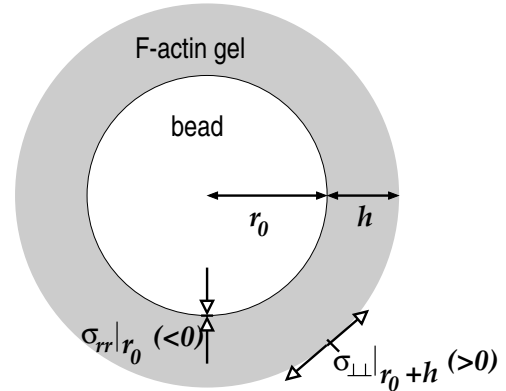

Fig. 2. The cross-section of the F-actin gel around a bead. The relevant stress components in the gel are schematically shown. The gel occupies the space between the radii $r = r_0$ and $r = r_0 + h$. The compressive component of the stress at the substrate surface ($r = r_0$), $\sigma_{rr}|_{r_0}$, and the tensile component at the outer surface ($r = r_0 + h$), $\sigma_{\perp\perp}|_{r_0+h}$, are indicated by the pairs of oppositely oriented open arrows. In this symmetric state, the tensile component at the substrate surface, $\sigma_{\perp\perp}|_{r_0}$, as well as the normal compressive component at the outer surface, $\sigma_{rr}|_{r_0+h}$, vanish.

These three ingredients i)-iii) constitute a positive feedback loop leading to an instability of the symmetric shape of the growing gel. This will be described in Section 5.1. In short, the region of gel with smaller thickness becomes preferentially dissociated due to the higher tensile stress, implying further thinning of that region.

All symmetry-breaking models [9,10] take the mechano-chemical coupling into account. Previous models have focused their attention on the compressive force acting on the actin filaments at the polymerization sites, that is on the substrate surface. Our analysis takes into account the global stress distribution. Of particular importance is the tensile stress generated at the outer surface of the gel. Indeed, on general grounds, the depolymerization rate must be an increasing function of the tensile stress. We show in the following that it leads inevitably to symmetry breaking. In the discussion section (Sect. 6), after a brief summary, we compare, in more details our analysis with the existing ones, and suggest experiments designed for distinguishing between the different possibilities.

2 Distribution of stress within the gel with symmetric shapes

Suppose that a gel has been polymerized steadily from a substrate surface of either spherical or cylindrical shape with radius r_0, until the gel forms a layer of a thickness h, enclosing the substrate surface and keeping its symmetry (see, Fig. 2). As already noted, the part of the gel that has been formed has been continuously pushed outwards. An element of the gel at radius r is then stretched by r/r_0 times relative to the native state of polymerization.

To know the tensile stress in the lateral direction, $\sigma_{\perp\perp}$, let us use the "stacked rubber band model" [5,11,12]: A

freshly cross-linked gel at the latex surface ($r = r_0$) is unstretched and has no lateral stresses, $\sigma_{\perp\perp}|_{r=r_0} = 0$. As the layer is pushed outward, its circumference increases which introduces a lateral stress [11],

$$\sigma_{\perp\perp}|_r = B\frac{r - r_0}{r_0}, \tag{1}$$

with B being the Young modulus. In particular, when the thickness of the gel layer is h, the tangential stress at the outer surface of the gel is

$$\sigma_{\perp\perp}|_{r_0+h} = B\frac{h}{r_0}. \tag{2}$$

We remark that the present approximation ignores the radial deformation due to the lateral stretching, in other words, it assumes a vanishing Poisson ratio. Although this has no justification for actin gels, the main results of the present paper do not depend on this property. More refined calculation confirm the validity of this statement [13].

The shear component of the stress $\sigma_{r\perp}$ vanishes everywhere, for symmetry reasons:

$$\sigma_{r\perp} = 0.$$

Radial force balance requires that the radial stress, σ_{rr}, at radius r obeys the following equations:

$$\frac{1}{r^2}\frac{\partial}{\partial r}\left(r^2\sigma_{rr}\right) - \frac{2}{r}\sigma_{\perp\perp} = 0 \tag{3}$$

for a spherical surface ([5], see App. A), or

$$\frac{\partial}{\partial r}\left(r\sigma_{rr}\right) - \sigma_{\perp\perp} = 0 \tag{4}$$

for a cylindrical surface [11]. Since no external force is applied on the outer surface of the gel layer, the normal stress must vanish:

$$\sigma_{rr}|_{r_0+h} = 0. \tag{5}$$

Under this condition, the normal stress at the substrate surface, $\sigma_{rr}|_{r_0}$, can be calculated in terms of the lateral stress, $\sigma_{\perp\perp}$. In the case of cylindrical substrate, we integrate equation (4) from $r = r_0$ to $r = r_0 + h$, and have

$$\sigma_{rr}|_{r_0} = -\frac{T}{r_0}, \tag{6}$$

where T is the *integrated tension* across the symmetric gel slab, defined by

$$T = \int_{r_0}^{r_0+h} \sigma_{\perp\perp}\,\mathrm{d}r. \tag{7}$$

Using equation (1) we find $T = Bh^2/(2r_0)$, and thus $\sigma_{rr}|_{r_0} = -Bh^2/(2r_0^2)$. For the spherical substrate, the relation is not as simple as the cylindrical case. Still, σ_{rr} is given as an integration of $\sigma_{\perp\perp}$.

3 Concentration of the tensile stress under a modulated surface profile

In this section, we consider how small perturbations to the surface profile of the gel layer lead to the redistribution of the stress components within the gel layer. We introduce the function representing the thickness of the gel layer, $h(\hat{\omega})$, with the variable $\hat{\omega}$ representing the orientation from the origin. A spherically symmetric gel layer corresponds to the constant function, $h(\hat{\omega}) = h^*$, with a constant thickness h^*.

The analysis of the thickness perturbation is done in the following two steps: In the first step, we suppose that this function, $h(\hat{\omega})$, is slightly perturbed from a constant function, but we still do not allow for the displacement of the gel. In the second step, we let the gel layer relax until it re-establishes the mechanical balance. We calculate how the stress in the gel is distributed in this new balanced state. To avoid any confusion, we stress that, the perturbations ($h(\hat{\omega}) - h^* \neq 0$) at the end of the first step does *not* imply the swelling or deswelling of the gel layer. The perturbation rather implies that there is more or less material of gel along the direction $\hat{\omega}$ than the average. (It could be due to the enhanced/depressed polymerization, or, to the depressed/enhanced dissociation of the gel along this direction.) As we discuss a situation such that there is no external force on the outer surface, we require stress-free conditions on the outer surface of the gel layer.

$$\sigma_{rr}|_{r_0+h} = \sigma_{r\perp}|_{r_0+h} = 0. \tag{8}$$

What we demonstrate is that, under the above conditions, the tensile stress $\sigma_{\perp\perp}$ under the re-established mechanical balance is locally enhanced in the thinned region of the gel layer, that is, in the zone of the orientation $\hat{\omega}$ that satisfies $h(\hat{\omega}) < h^*$. On the one hand, the physical origin of the stress concentration is quite simple and universal. In fact the authors have noticed, after completion of the present work, that essentially the same mechanism of stress concentration has been discussed long before in the context of crystal growth under stress (see, for example, a concise review on the related history in the literature [14]). In Appendix B we describe the basic mechanism of this phenomenon by using an illustrating example in a very simple geometry. On the other hand, the direct analysis of the present case with the distributed thickness $h(\hat{\omega})$ is difficult, because of the three spatial dimensionalities and the tensorial character of the stress associated to this space. We can avoid, however, this difficulty by the following lines of reasoning.

1) We limit our concern to the modulations $h(\hat{\omega}) - h^*$ whose characteristic wavelengths are comparable to the average thickness, h^*. Experimentally, h^*/r_0 is at most about 0.2 [15]. The radius of curvature of the outer surface ($\simeq r_0 + h^*$) is, therefore, not appreciable in view of such short wavelength of modulation. We may then ignore the effect of a specific curved geometry of the substrate surface *except for* the fact that the curvature gives rise to the lateral tension $\sigma_{\perp\perp}$ in the gel layer.
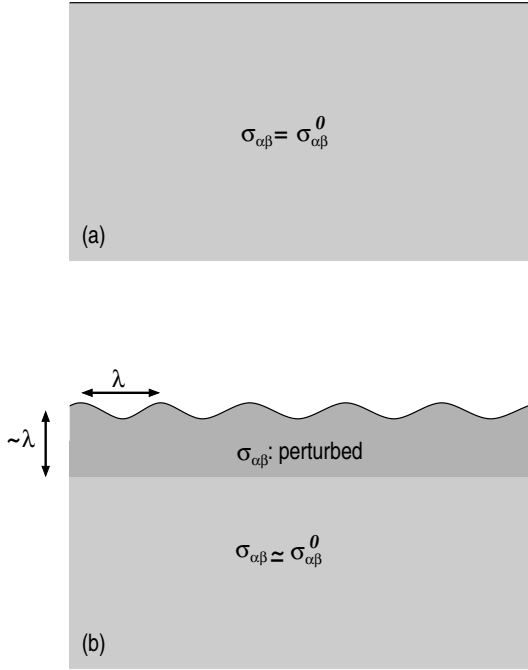
Fig. 3. Schematic representation of the outer gel surface before (a) and after (b) perturbation. A perturbation of the surface profile with characteristic length λ affects the stress profile only within a "skin layer" of thickness λ.

2) We notice the following fact: As far as the stress distribution inside the gel layer is concerned, the influence of the surface profile perturbation is practically limited to a region near the outer surface (see, Fig. 3). More precisely, if the perturbation is characterized by a wavelength, λ, then the thickness of the disturbed region is also characterized by λ. (The boundary condition far from this layer is therefore irrelevant to this disturbance.) For detailed arguments, see Appendix C.

3) With our wavelength choice in 1), and with the fact just mentioned above 2), we can justify the study of a) a two-dimensional circular geometry rather than the real spherical one, with b) a "slip" boundary condition on the substrate surface, to see how the stress in the actual three-dimensional case is distributed after the re-establishment of the mechanical balance. Moreover, c) the neglect of the shear stress components within the gel layer is justifiable for the experimentally realized situation where the mean thickness of the gel layer h^* is much smaller than the radius r_0. We will formulate these assumptions in more details below.

a) *We consider the gel layer grown around a two-dimensional circle of radius r_0.*
   In two dimension, we represent the thickness of the gel layer by $h(\theta_0)$ as a function of the angle θ_0 with $0 \leq \theta_0 < 2\pi$, instead of $h(\hat{\omega})$ above. (See, Fig. 4: $h(\theta_0)$ is defined *before* the re-establishment of the mechanical balance.) The lateral components of the stress, which we have denoted symbolically by $\perp$, corresponds now to the azimuthal direction. We then use the suffix θ in place of $\perp$ hereafter. For example, we write $\sigma_{r\theta}$ for
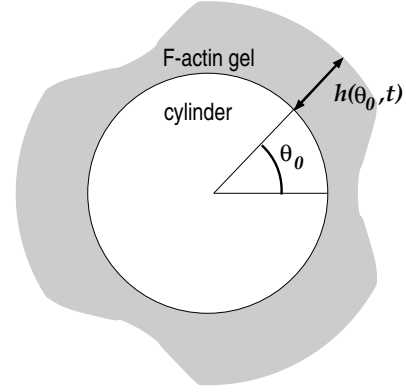

Fig. 4. Definition of the angler variable θ_0 and the height function $h(\theta_0)$ of a gel with modulated thickness due to depolymerization before an elastic deformation re-establishes mechanical equilibrium.

$\sigma_{r\perp}$, and $\sigma_{\theta\theta}$ instead of $\sigma_{\perp\perp}$. For small perturbations of the thickness, $|h(\theta_0) - h^*|/h^* \ll 1$, we may use the linear analysis. Then it suffices to consider the form

$$h(\theta_0) = h^* \left[1 + \epsilon_q \cos(q\,\theta_0)\right], \qquad (9)$$

where the integer q indicates the number of nodes of the spatial undulations, and ϵ_q is supposed to be small ($|\epsilon_q| \ll 1$). The characteristic wavelength for the q-th mode is about $2\pi r_0/q$, and the restriction (1) is represented as $q \simeq \frac{2\pi r_0}{h^*}$. (Remark: Besides our purpose of analysis, the two-dimensional geometry applies rather directly to a *Listeria* mutant [8] mentioned in Sect. 1. This mutant moves preferentially in lateral directions, breaking its cylindrical symmetry.)

b) *On the substrate surface $(r = r_0)$, the shear stress is negligible.*
   The slip boundary condition for the shear stress is written as

$$\sigma_{r\theta}\big|_{r_0} = 0. \qquad (10)$$

   (Remark: Note that we do not claim this boundary condition to be always realistic. We rather use this condition since it is justifiable for the calculation of the stress distribution under the modes of perturbations with $q \simeq \frac{2\pi r_0}{h^*}$: See argument 2) above and App. C for details.)

c) *The shear stress $\sigma_{r\theta}$ within the gel layer is negligible.*
   As mentioned above, the experimental value of h^*/r_0 is $\ll 1$. In such situation we may, in the lowest-order approximation, estimate the magnitude of the shear stress, with a parabolic profile of the shear stress $\sigma_{r\theta}$: $\sigma_{r\theta} = \tilde{\mu}\epsilon_q(r_0 + h - r)(r - r_0)/r_0^2$ for $r_0 \leq r \leq r_0 + h$, which satisfies the boundary conditions, equations (8) and (10). Here, $\tilde{\mu}$ is a constant proportional to the shear modulus μ of the gel. The magnitude of $\sigma_{r\theta}$ is, therefore, at most of the order of $\tilde{\mu}\epsilon_q(h^*/r_0)^2$. We compare this with the change of $\sigma_{\theta\theta}$ due to the perturbations of the thickness, which is of order $\epsilon_q B h^*/r_0$ (see

Eq. (1)). Then $\sigma_{r\theta}$ is smaller than this by a factor of h^*/r_0, and is therefore negligible.

In Appendix D we show how the stress distribution within the gel is calculated for the model described by a)-c). Below, we show only the results for the tensile stresses $\sigma_{\theta\theta}|_{r_0+h}$ at the external gel surface and the normal compression, $-\sigma_{rr}|_{r_0}$ at the substrate surface:

$$\sigma_{\theta\theta}|_{r_0+h} - \left(\sigma_{\theta\theta}|_{r_0+h}\right)_{\epsilon_q=0} = -\frac{B\chi^2}{2+\chi}\epsilon_q \cos(q\,\theta_0) + \mathcal{O}(\epsilon_q^2), \tag{11}$$

$$-\sigma_{rr}|_{r_0} - \left(-\sigma_{rr}|_{r_0}\right)_{\epsilon_q=0} = \mathcal{O}(\epsilon_q^2), \tag{12}$$

with $\chi \equiv h^*/r_0$. The bracketed terms with the subscript $\epsilon_q = 0$ are those terms without perturbation: $\left(\sigma_{\theta\theta}|_{r_0+h}\right)_{\epsilon_q=0} = B\chi$ and $\left(-\sigma_{rr}|_{r_0}\right)_{\epsilon_q=0} = \frac{B}{2}\chi^2$ (see Eqs. (2) and (6)). In equation (12), $\mathcal{O}(\epsilon_q^2)$ indicates the terms of at least second order of ϵ_q. Since $\epsilon_q \cos(q\,\theta_0) = (h(\theta_0) - h^*)/h^*$, the minus sign on the right-hand side of equation (11) implies that the lateral tension is augmented, $\sigma_{\theta\theta}|_{r_0} > \left(\sigma_{\theta\theta}|_{r_0}\right)_{\epsilon_q=0}$, in the thinned portion of the layer, $h(\theta_0) < h^*$.

4 Mechano-chemical coupling: Growth and dissociation of gel under stress

In this section, we consider the time evolution of the thickness of the gel layer. We denote the profile of the thickness at the time t as $h(\theta_0, t)$. We are interested in the chemical processes which take place on time scales much larger than the establishment of the mechanical balance within the gel. We suppose that the relevant microscopic chemical processes are the polymerization and branching of the actin filaments to form the gel, and the unbinding of the branching points and/or through the depolymerization of actin filaments to dissociate the gel. We adopt a simplified version of the model proposed previously [15,5]:

$$\frac{\partial h(\theta_0, t)}{\partial t} = a\left[\bar{k}_{\rm p} e^{\sigma_{rr}|_{r_0} c_{\rm p}} - k_{\rm d} e^{\sigma_{\theta\theta}|_{r_0+h(\theta_0,t)} c_{\rm d}}\right], \tag{13}$$

where a, $\bar{k}_{\rm p}$, $k_{\rm d}$, $c_{\rm p}$ and $c_{\rm d}$ are positive constants. The prefactor a outside the square bracket on the right-hand side (r.h.s.) is a length of about the size of an actin monomer. This represents the rate of conversion between the chemical processes and the change of the thickness, h. The other parameters are described below.

In the square bracket on the right-hand side (r.h.s.) of equation (13), the first term represents the polymerization at the substrate surface ($r = r_0$). Here, we have introduced the assumption: i) *On the substrate surface, the polymerization is the dominant process.* The pre-exponential factor $\bar{k}_{\rm p}$ represents the kinetic constants in the absence of compressive stress ($\sigma_{rr}|_{r_0} = 0$). $\bar{k}_{\rm p}$ depends on the concentration of actin monomers in the solvent. In our analysis we assume this to be constant. The exponential factor represents the fact that the polymerization is decelerated

by the compression, $\sigma_{rr}|_{r_0}$ (< 0). The parameter $c_{\rm p}$ has been introduced so that $-c_{\rm p}\,\sigma_{rr}|_{r_0}$ accounts for the increase in the polymerization potential barrier due to the cost in elastic energy (divided by $k_{\rm B}T$) to push out the gel layer outward against the compressive stress. We have neglected the dissociation of the gel at the substrate surface. Such process could be easily incorporated in the model [16,13], but has little effect in our context. In the experiment of the polymerization of microtubules, it has been shown that the negligence of the depolymerization on the growing end (the plus end) is a good approximation [17].

The second term in the square bracket on the r.h.s. of equation (13) represents the gel dissociation. We have introduced the assumption: ii) *The dissociation process is almost localized on the outer surface of the gel at* $r = r_0 + h(\theta_0, t)$. The pre-exponential factor, $-ak_{\rm d}$, therefore represents the rate of thickness decrease which occurs due to the dissociation of the gel under the stress-free condition, $\sigma_{\theta\theta}|_{r_0+h(\theta_0,t)} = 0$. (Remark: Here we can identify $\sigma_{\theta\theta}|_{r_0+h(\theta_0,t)}$ as the tensile stress along the tangent of the outer surface, since the correction is of second order of the deviation angle, $|\frac{\partial h}{\partial \theta_0}|/(r_0 + h)$, between the tangential direction and the azimuthal direction.) The exponential factor of this term represents the fact that the dissociation is accelerated by the lateral tensile stress $\sigma_{\theta\theta}|_{r_0+h(\theta_0,t)}$ (> 0). The parameter $c_{\rm d}$ has been introduced so that $c_{\rm d}\,\sigma_{\theta\theta}|_{r_0+h(\theta_0,t)}$ accounts for decrease in the depolymerization potential barrier due to the release of the elastic energy (divided by $k_{\rm B}T$) when the gel is dissociated under the tensile stress. We have neglected the dissociation of the gel occurring inside the gel. There are good reasons to believe that the gel dissociation is strongly accelerated under tensile stress [16], as compared with spontaneous dissociation under the stress-free condition. In fact, the experiments using the full cell extract as the solvent have shown that the mean thickness of the gel layer around the latex bead is much smaller than the average length of the comet produced by *Listeria* of similar size. It implies that the Boltzmann factor of the form, $e^{c_{\rm d}\sigma_{\theta\theta}}$, is crucial to determine the dissociation rate. As $\sigma_{\theta\theta}$ is largest on the outer surface of the gel, we suppose that the gel dissociation occurs mostly in the vicinity of the outer surface.

The kinetic equation, equation (13), also assumes the following: iii) *The diffusion of actin monomer is fast enough.* This limits our analysis to a bead radius range smaller than a cross-over size, $r_{\rm c}$, separating a stress-governed regime from a diffusion-controlled regime. Indeed, on the substrate surface, the actin gel is formed from the adjunction of actin monomer molecules. And for these molecules to reach the substrate surface, they have to diffuse through the network of the actin gel. Previous experimental and theoretical analysis [5] indicates that, as far as the diameter of the latex bead is less than about $5\ \mu$m, and under physiological concentrations of the actin monomers and of the cross-linker molecules, diffusion does not limit the thickness evolution, $h(\theta_0, t)$.

The evolution equation, equation (13), has a solution corresponding to the symmetric stationary state, $h(\theta_0, t) = h^*$ [5]. If we restrict our analysis to the circularly

symmetric profiles, $h(\theta_0, t) = h(t)$, this solution is *stable*. In fact, substituting the form $h(\theta_0, t) = h^*$ into equation (13), we obtain the equation for $\chi \equiv h^*/r_0$ as

$$\frac{c_{\rm p}}{c_{\rm d}} \chi^2 + \chi - \frac{2}{c_{\rm d} B} \log\left(\frac{\bar{k}_{\rm p}}{k_{\rm d}}\right) = 0. \qquad (14)$$

This equation has a positive, therefore, physically meaningful, solution for $\bar{k}_{\rm p}/k_{\rm d} > 1$, Furthermore, if we substitute the form

$$h(\theta_0, t) = h^* \left[1 + \epsilon_0(t)\right], \qquad (15)$$

equation (13) reduces, up to linear order in $\epsilon_0(t)$, to the following equation:

$$\frac{{\rm d}\epsilon_0(t)}{{\rm d}t} = -\frac{\epsilon_0(t)}{\tau_0}, \qquad (16)$$

with $\tau_0 = k_{\rm d}^{-1} \Omega_0^{-1} r_0/a$,

$$\Omega_0 = c_{\rm d} B e^{c_{\rm d} B \chi}\left(1 + \frac{c_{\rm p}}{c_{\rm d}}\chi\right). \qquad (17)$$

Equation (16) shows, as already mentioned, that the steady-state solution $h(\theta_0, t) = h^*$ is stable with respect to perturbations keeping the overall symmetry. This result is understandable since a radius with $h > h^*$ ($< h^*$) would lead to an increase (decrease) of both $(-\sigma_{rr}|_{r_0})$ and $\sigma_{\perp\perp}|_{r_0+h}$, and these in turn make the r.h.s of equation (13) negative (positive), leading to a decrease (increase) of h toward the stationary value h^*. From equations (14) and (17), χ and τ_0 are functions of three parameters, $c_{\rm d} B$, $\frac{c_{\rm p}}{c_{\rm d}}$, and $\frac{\bar{k}_{\rm p}}{k_{\rm d}}$. Note that τ_0 is a few orders of magnitude larger than the microscopic time $k_{\rm d}^{-1}$, with r_0/a being of order 10^3 and Ω_0 of order 10.

5 Result

5.1 Symmetry-breaking instability

We now consider symmetry-breaking perturbations and we assume the following form for the gel layer profile:

$$h(\theta_0, t) = h^* \left[1 + \epsilon_q(t) \cos(q\,\theta_0)\right], \qquad (18)$$

with $q \neq 0$. Substituting the expressions of the stress components, equations (11) and (12) into equation (13), where ϵ_q is replaced by $\epsilon_q(t)$, we have the following equation up to the linear order of $\epsilon_q(t)$,

$$\frac{{\rm d}\epsilon_q(t)}{{\rm d}t} = \frac{\epsilon_q(t)}{\tau_q}, \qquad (19)$$

with $\tau_q = \tau_0 \frac{\Omega_0}{\Omega_q}$,

$$\Omega_q = c_{\rm d} B \, e^{c_{\rm d} B \chi} \frac{\chi}{2 + \chi}, \qquad (20)$$

where $\chi \equiv h^*/r_0$ as before. (Remember that χ can be expressed in terms of the parameters $c_{\rm d} B$, $\frac{c_{\rm p}}{c_{\rm d}}$, and $\frac{\bar{k}_{\rm p}}{k_{\rm d}}$.) Note that since $\Omega_0 \Omega_q \simeq 2/\chi \simeq 10$, $\tau_0 \ll \tau_q$. Equations (19) and (20) imply the following characteristics of the symmetric stationary state $h(\theta_0, t) = h^*$.

i) *The symmetric stationary state is unstable against perturbations which break the symmetry*, since all τ_q are positive. In fact, the applicability of our model is guaranteed only in the range of q satisfying $q \simeq \frac{2\pi r_0}{h^*}$ (see, Sect. 3). Nevertheless, the presence of *an* unstable mode is sufficient for the proof of instability. Note also that since $\tau_0 \ll \tau_q$, our analysis predicts that a quasi-symmetric steady state should be reached significantly earlier than the onset of symmetry breaking. This is indeed what is observed.

ii) *The characteristic time of the instability is proportional to the radius of the substrate if the other parameters are fixed*. It is reasonable to suppose that τ_q represents the characteristic time of the growth of the perturbation. Then, from (19), τ_q is written in a scaling form:

$$\frac{\tau_q}{k_{\rm d}^{-1}} = \Omega_q^{-1} \frac{r_0}{a}, \qquad (21)$$

where $k_{\rm d}^{-1}$ and a play the role of intrinsic time scale and length scale, respectively. The dimensionless constant of proportionality, Ω_q^{-1}, depends on the properties of the gel and of the solvent through the parameters, $c_{\rm d} B$, $\frac{c_{\rm p}}{c_{\rm d}}$, and $\frac{\bar{k}_{\rm p}}{k_{\rm d}}$. Note that, in fact, the quantity τ_q thus defined shows no dependence on $q(\neq 0)$, as Ω_q does not. This apparently anomalous behavior should not be taken seriously, because the range of wave number validity of our analysis is limited to $q \simeq \frac{2\pi r_0}{h^*}$.)

Quantitatively, we can evaluate the characteristic time τ_q using the experimentally known data in the literature: The stationary velocity $v_{\rm gel}$ at which the gel material moves outward is identified from equation (13) as

$$v_{\rm gel}/r_0 = k_{\rm d}(a/r_0) e^{c_{\rm d}\,\sigma_{\theta\theta}|_{r_0+h(\theta_0,t)}} = k_{\rm d}(a/r_0) e^{c_{\rm d} B \chi}.$$

Comparing this with the expression of τ_q obtained from equations (20) and (21), $\tau^{-1} = k_{\rm d}(a/r_0)\,e^{c_{\rm d} B \chi}\,c_{\rm d} B \chi/(2 + \chi)$, we see that

$$\tau = \frac{r_0}{v_{\rm gel}} \frac{2 + \chi}{c_{\rm d} B \chi}. \qquad (22)$$

As described in [5], $c_{\rm d} B \chi$ is the decrease in energy barrier (in units of $k_{\rm B} T$) in the dissociation of an actin filament under tensile stress, compared to the unstressed case. For the effects described in this manuscript to be observable, this decrease must be of order one. Noting that $\chi \ll 2$, our analysis requires the combination $\tau_q v_{\rm gel}/(2r_0)$ to be of order one. The experiment gives $\tau_{\rm sym}/r_0 \simeq 5$ min/μm and $v_{\rm gel} \simeq 1\mu$m/min (note that it is the polymerization rate under stress) which leads to $\tau_q v_{\rm gel}/(2r_0) \simeq 2.5$. This is in the expected range.

5.2 Role of external symmetry-breaking perturbations

In reality, a strictly symmetric substrate, either spherical or cylindrical, is impossible. Also, the chemical properties of the substrate surface are never perfectly homogeneous. A nominally spherical latex bead may contain a weak local deviation of the surface curvature and a weak heterogeneity of the polymerization constant, $\bar{k}_{\mathrm{p}}$, along the surface. Thus, we should suppose that there are disturbances which break *externally* the symmetry of the system, and modify equation (13) or its linearized form, equation (19). A legitimate question is, therefore, "if and how the above symmetry-breaking *instability* plays a role?" In short, the answer is that, despite these extrinsic factors, the instability mechanism of symmetry breaking manifests itself in the evolution of the gel's thickness, justifying our comparison with experiments done in the above Section 5.1 We discuss it first in a formal manner, and then in the context of the geometrical and chemical heterogeneities.

Within the linear approximation, the evolution equation, equation (13), is decomposed into the equation for each mode, like equations (16) or (19). In the latter equation the system's intrinsic heterogeneity may be represented as a small but finite source term, ϵ_q^{e},

$$\frac{\mathrm{d}\epsilon_q(t)}{\mathrm{d}t} = \frac{1}{\tau_q}(\epsilon_q(t) + \epsilon_q^{\mathrm{e}}). \tag{23}$$

We can solve this equation with the initial condition $\epsilon_q(0) = 0$:

$$\epsilon_q(t) = \epsilon_q^{\mathrm{e}}\tau(e^{\frac{t}{\tau}} - 1) \simeq \begin{cases} \epsilon_q^{\mathrm{e}}/\tau_q t, \text{ for } t < \tau \\ \epsilon_q^{\mathrm{e}} e^{\frac{t}{\tau}}, \text{ for } t > \tau \end{cases}. \tag{24}$$

This shows that, after a time $t \sim$ a few τ, the effect of the non-symmetric disturbance is exponentially amplified $(e^{t/\tau} \gg 1)$ by the instability mechanism, while the direct effect of the source is small in the sense that $\epsilon_q^{\mathrm{e}} t \ll 1$ even for $t \simeq$ few τ_q. In this way, the symmetry-breaking mechanism manifests itself as an amplifier of small heterogeneous disturbance in the system, which can be experimentally observable.

Another way to think about the external perturbation is to define the time $\tau_{\mathrm{S}q}$ required for developing an ϵ_q of a specified value ϵ_q^{S}: Equation (24) leads to

$$\tau_{\mathrm{S}q} = \tau_q \ln\left(1 + \frac{\epsilon_q^{\mathrm{S}}}{\epsilon_q^{\mathrm{e}}}\right). \tag{25}$$

Changing the prescribed value ϵ_q^{S} or the external perturbation ϵ_q^{e} by orders of magnitude changes τ_{S} only by a small factor. This tells us that, as already announced, the scaling of the characteristic observable times is essentially given by τ_q. It also tells us that the detailed knowledge of the early dynamics is not essential in the definition of $\tau_{\mathrm{S}q}$ provided τ_q is sufficiently larger than τ_0, so that a quasi-spherical state is obtained before the symmetry-breaking process is observed. We know this to be true both from our analysis and from experiment.

Now we describe how the parameter ϵ_q^{e} reflects the effect of the heterogeneity of the surface curvature and of the polymerization rate. Under the linear approximation, we only need to consider the profile of the substrate surface which can be described in terms of the radius $r_0(\theta_0)$ as a function of the angle θ_0: $r_0(\theta_0) = r_0 + \Delta_q^{\mathrm{(geo)}}\cos(q\theta_0)$. Additionally, we consider the spatial distribution of the polymerization rate constant $\bar{k}_{\mathrm{p}}$ represented as a function of θ_0: $\bar{k}_{\mathrm{p}}(\theta_0) = \bar{k}_{\mathrm{p}0} + \Delta_q^{\mathrm{(chem)}}\cos(q\theta_0)$. $\Delta_q^{\mathrm{(geo)}}$ and $\Delta_q^{\mathrm{(chem)}}$ characterize the amplitudes of geometrical and chemical perturbations, respectively. The geometric profile $r_0(\theta_0)$ leads to the non-homogeneous curvature $\kappa(\theta_0)$, which has the following form:

$$\kappa(\theta_0) = \frac{1}{r_0}\left[1 + \frac{\Delta_q^{\mathrm{(geo)}}}{r_0}(q^2 - 1)\cos(q\theta_0)\right].$$

Along the line of calculation in Appendix D, this expression of the curvature should replace the factor r_0^{-1} in equation (D.7). The normal stress on the substrate surface is therefore given by

$$\sigma_{rr}|_{r_0} = -\kappa(\theta)T. \tag{26}$$

As for the chemical heterogeneity in the polymerization rate, $\bar{k}_{\mathrm{p}}(\theta_0)$ should replace $\bar{k}_{\mathrm{p}}$ in equation (13). In general, these effects can be summarized in the form of $\epsilon_q^{\mathrm{e}} = \beta_q^{\mathrm{(chem)}}(\Delta_q^{\mathrm{(chem)}}/\bar{k}_{\mathrm{p}}) + \beta_q^{\mathrm{(geo)}}(\Delta_q^{\mathrm{(geo)}}/r_0)$, with dimensionless numbers $\beta_q^{\mathrm{(chem)}}$ and $\beta_q^{\mathrm{(geo)}}$. However, if these source terms have existed from the start of polymerization, the expressions of $\beta_q^{\mathrm{(chem)}}$ and $\beta_q^{\mathrm{(geo)}}$ are complex because in the early stages of the gel growth none of the linear equation is valid. However, as we have already pointed out the exact knowledge of ϵ_q^{e} is not essential for understanding the main feature of the dynamics if $\tau_0 < \tau_q$. We, therefore, only mention about the restricted case where those heterogeneities are switched on at a certain moment of time after the symmetric steady state has been established. The result then reads

$$\epsilon_q^{\mathrm{e}} = \frac{e^{c_{\mathrm{d}}B\chi}}{\Omega_q\chi}\left(\frac{\Delta_q^{\mathrm{(chem)}}}{\bar{k}_{\mathrm{p}}} - \frac{c_{\mathrm{p}}B\chi^2}{2}(q^2 - 1)\frac{\Delta_q^{\mathrm{(geo)}}}{r_0}\right). \tag{27}$$

The positive coefficient in front of $\Delta_q^{\mathrm{(chem)}}$ reflects the acceleration of the turnover of the gel material where $\bar{k}_{\mathrm{p}}$ is increased, while the minus sign in front of the second term in the bracket reflects the polymerization being slowed down where the surface extrudes, or, where $\kappa(\theta_0) > \frac{1}{r_0}$.

6 Discussion

Our analysis based on gel elasticity leads to the essential prediction that the spherical symmetry is always unstable. The expected scenario is that in a first step a quasi-spherical steady state is reached which should obey the prediction contained in [5] and [18]. Then on a time scale

significantly larger than the characteristic time for reaching the isotropic quasi-steady state, symmetry is broken. In the regime we discuss, governed by elasticity, these two times are predicted to scale like the radius of the bead on which the experiment is conducted. This scaling should be very robust in the elastic regime, since r_0 is the only length scale in the problem. In particular, it should hold for wavelengths larger than those considered here. All these expectations are well born out by experiment [7]. In a number of cases symmetry is not observed to be broken: this may be due to three different causes: 1) the experiment duration might not be long enough for the symmetry-breaking event to take place, 2) the gel/bead friction, considered in Appendix E might further slow down the symmetry-breaking process, 3) the gel might not behave fully elastically at very long time scales. In this latter case, a new time scale would come into play, namely that over which a significant stress may be maintained, and a new calculation should be developed. We discuss various possible improvements to our current analysis in Appendix E.

As explained in this manuscript the main ingredient for the occurrence of symmetry breaking comes from the tensile-stress concentration where the gel thickness is smallest. This feature, added to a stress-dependent depolymerization in the immediate vicinity of the gel outer surface, leads to an absolute instability of the system. This is in contrast with earlier models [9,10] in which symmetry is broken at the polymerizing gel bead surface. Their interpretation is most transparent in the one-dimensional case; consider two opposing sides on which parallel filaments are grown. The force on individual filaments, *i.e.* the ratio of the total force (equal on both sides because of force balance) to the number of supporting filaments, is the key notion. The smaller the number of filaments participating, the slower the effective polymerization rate; it is natural to expect a force dependence and different scenarios have been discussed [9,10] if an unbalance between the two sides arises at some point, it grows since the "weak" side tends to become "weaker". The two-dimensional version of this mechanism, simulated by van Oudenaarden *et al.* [9] is closely related to simulation and experiments done on the microtubule/centrosome (or microtubule/bead) system. The latter system does not exhibit an instability whereas the first does. The difference in behavior results from the difference in boundary conditions. All these cases do not consider the situation where filaments are cross-linked. Actin gels are cross-linked and we propose that in two and three dimensions these cross-links change profoundly the behavior. Indeed, if the thickness of the gel layer is locally decreased, the compressive stress there, $\sigma_{rr}|_{r_0}$, should either stay constant if full-slip boundary conditions are achieved, or decrease, irrespective of the thinning cause. The lateral displacement of the gel layer along the substrate surface might at most relax some of this local decrease of $\sigma_{rr}|_{r_0}$, but it will never be able to increase it. Thus, the mechanism described [9,10] for non-cross-linked filaments do not apply to gels.

There might be an objection here: admitting that the compressive stresses at the substrate surface can at most stay constant, would this not decrease the local filament density and therefore increase the compressive force per filament, exactly as proposed by van Oudenaarden *et al.* [9]? We could agree on this point if the rate of branching/cross-linking per filament were to be always constant, as it was assumed in the previous models by van Oudenaarden and Theriot [9] and by Mogilner and Oster [10]. In fact, however, the density of actin filaments on the substrate surface is likely to be insensitive to the lateral stretching of gel. The reason is, as is shortly discussed in Appendix E (item 7), that the growth of the gel proceeds in the way that the tensile stress is almost zero on the substrate surface. Therefore, the frequency of the branching and the resulting density of actin filaments on the surface should be determined by the compressional stress from the gel, which is *unchanged* up to the order of $\epsilon_q(t)$ (the amplitude of the perturbation) and by the density of the enzyme, which is supposed to be uniform on the surface, except in the discussion in Section 5.2. Of course the above argument is justifiable so long as the evolution of the symmetry breaking is not extremely fast compared with the microscopic characteristic time of branching.

A direct experimental assessment of the symmetry-breaking mechanism could involve monitoring simultaneously the depolymerization and the polymerization processes at the outer and inner gel surfaces, respectively. This is not an easy experiment.

In the present paper, we assumed that the degradation of gel occurs mainly through the depolymerization. However, the gel fracture would explain the symmetry breaking: In fact both the depolymerizatin scenario in our paper and the rupture scenario can be viewed as two extremes of a unified instability model. What is common to both scenarios is that spontaneous degradation of gel from the outer surface is supposed to exist even if there are no stretching stresses. The difference is the spatial patterns with which the symmetry is broken, either a smooth perturbation of the thickness or by a sharp wedge opening in the gel layer. (In the field of polymer physics, it is reminiscent of the two complementary models of microphase separation in diblock copolymers, called the models of strong segregation limit and of weak segregation limit, respectively.) In both cases, the degradation of gel should start from the external surface of the gel where the tensile stress is the strongest. As there are no direct experimental evidences that distinguishes the depolymerizatin from the rupture upon symmetry breaking, we have taken the former hypothesis to do a concrete analysis. It is also possible that the rupture appears as the late and non-linear stage of symmetry breaking which is initiated by a weak linear instability through inhomogeneous depolymerization.

Both models may explain the apparent absence of the breaking of symmetry around the beads with large diameter: The establishment of an appreciable tensile stress requires long time and thick gel layer for large diameter, as described in the text. Therefore, the diffusion of the monomer components of the gel (actin, Arp2/3 etc.) might become the limiting process of the gel growth [18]. As a result, the gel thickness attain a stationary value

independent of the diameter of the bead, as a balance between the the "evaporation" (spontaneous degradation of gel independent of the tensile stress) from the outer surface and the growth from the inner surface. In the rupture scenario, the symmetry breaking is suppressed by the inadequacy of the stretching stress to make fracture, while in the depolymerization sceanario the suppression is ascribed to the smallness of the tension-dependent degradation.

Finally, we would like to discuss about the plastic character of the actin gel. The actin gel under tension may show the plasticity in a particular sense: It is largely believed that Arp2/3, the cross-linker of the actin network, is incorporated to the network only on the sufrace where the enzymes (fragments of WASP or ActA) for this reaction can be activated. In the bulk of the gel the loss of the cross-linking, therefore, takes place in an irreversible manner with no recovery process of cross-linking. Thus, this process of plasticity in actin gel is mostly equivalent to the hypothesis of depolymerization of our model, and it should therefore be distinguished from the viscoelasticity of Maxwell or Voigt models in which the elastic aspect is not lost irreversibly. Though we have not looked at the plasticity aspect of actin gel entirely in detail, since the plasticity is not an absolutely necessary approach or viewpoint for the purpose of the symmetry breaking. Still, we think that the plasticity could be an interesting subject to be studied more in future. To the authors' knowledge, there have been no studies about the plasticity of actin gel up to the present time.

Appendix A. Heuristic derivation of the equations of mechanical balance

Equations (3) and (4) in Section 2 are the equation of mechanical balance of stress components in the spherically and circularly symmetric geometries, expressed in respective relevant coordinate systems. Instead of deriving these from the familiar form in the Cartesian coordinates (symbolically written as $\nabla \cdot \sigma = 0$) through coordinate transformations, we will present an elementary physical interpretation of the equations of mechanical balance. It might help to understand how the lateral tensile stress and the normal compressive stress are related. See, Figure 5. Consider, within a layer of actin gel occupying the radii r_0 and $r_0 + h$, a slice of gel between the radii r and $r + \Delta r$ spanning a solid angle $\Delta\Omega$ (3D) or an angle θ (2D). The lateral tension $\sigma_{\perp\perp}$ gives an effective surface tension $\Delta\Gamma = \sigma_{\perp\perp}\Delta r$ to this slice. Because of the curvature radius, r, of this slice, a sort of the Laplace pressure, $2\Delta\Gamma/r$ (3D) or $\Delta\Gamma/r$ (2D) is generated towards the center ($r = 0$) of curvature. This pressure integrated over the surface, $r^2\Delta\Omega$ (3D) or $r\Delta\theta$ (2D), gives the total force
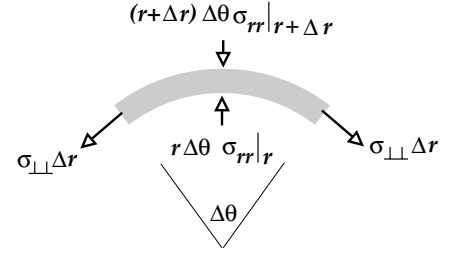

Fig. 5. Forces acting on a curved slice of gel of thickness Δr and length $r\Delta\theta$. The slice is under lateral tension because of forces $\sigma_{\perp\perp}\Delta r$. It is radially compressed because of the forces $(r + \Delta r)\Delta\theta\ \sigma_{rr}|_{r+\Delta r}$ and $r\Delta\theta\ \sigma_{rr}|_r$.
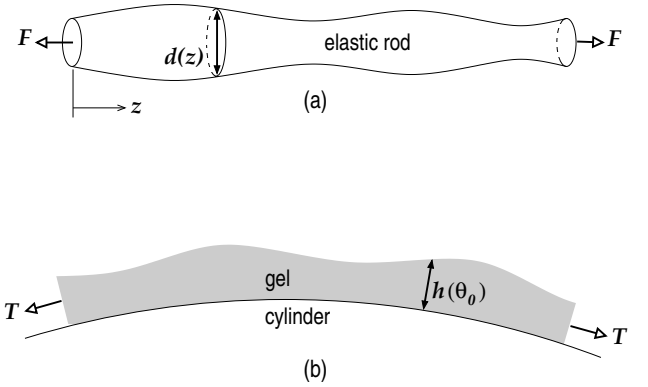

Fig. 6. Stress distribution in elastic structures of varying thickness: (a) Elastic rod of thickness $d(z)$ under tension due to forces F acting at the ends. The tension at coordinate z: $\sigma_{zz} \simeq F/A(d)$, where $A(d) = \frac{\pi}{4}d(z)^2$. (b) Analogous situation in a gel layer of thickness $h(\theta_0)$ under integrated tension T. The tensile stress can be approximated as $\sigma_{\perp\perp} \simeq \frac{T}{h(\theta)}$.

exerted by this thin layer. These force in the respective dimensionality are shown on the right-hand side of the equations below. Now, these forces must be the origin of the difference between the integrated normal stress acting at r and that at $r + \Delta r$. The differences in the respective dimensionality are shown on the left-hand side of the equations below:

$$(r+\Delta r)^2\Delta\Omega\sigma_{rr}|_{r+\Delta r}-r^2\Delta\Omega\sigma_{rr}|_r=r^2\Delta\Omega\frac{2\sigma_{\perp\perp}\Delta r}{r}, \quad (3D)$$

$$(r+\Delta r)\Delta\theta\sigma_{rr}|_{r+\Delta r}-r\Delta\theta\sigma_{rr}|_r=r\Delta\theta\frac{\sigma_{\perp\perp}\Delta r}{r}, \quad (2D)$$

Dividing both hand sides of the above equations by Δr, and letting $\Delta r \to 0$, we arrive at equations (3) and (4). Note that $\sigma_{rr} < 0$ for compressive stresses.

Appendix B. Elementary physical mechanism of the stress concentration

We describe the basic mechanism of the stress concentration by an illustrating example with a very simple geometry (see, Fig. 6(a)).

Suppose that there is a long elastic rod whose diameter $d(z)$ is inhomogeneous along its long axis, z. We now apply a tensile force to this rod by pulling its ends apart. Once the balance of force is re-established within the rod, the total tensile force integrated over a sectional plane perpendicular to the z-axis is constant along the z-coordinate. Thus, the tensile stress σ_{zz} averaged over this section is inversely proportional to its area, $\pi(d(z)/2)^2$. By such geometrical effect, the tensile stress is concentrated at the thinnest part of the rod.

We could mention an analogous situation in an electric wire transporting a steady electric current. If the thickness of the wire is inhomogeneous, the electronic-current *density* is high in the region where the wire is thin, by the same geometrical effect. The electric-current density plays the role of the tensile stress σ_{zz} in the former case. In fact, the stress is the current density of the momentum [12].

We may compare these quasi–one-dimensional examples with the geometry studied in Section 3 (see Fig. 6(b)). In the latter situation, the gel is under lateral tensile force T. By the same reasoning as above, the lateral tensile stress is large where the thickness is small. Although the shear force between the gel and the cylinder would weaken this effect, the basic mechanism still works.

The geometrical effect discussed here is quite universal: We only need a current density of some physical quantity (*e.g.*, the momentum, the charge, etc.) which is confined along some direction(s).

Appendix C.

We demonstrate that the perturbations of the surface profile have a limited influence on the stress, practically confined within a "skin depth" near the outer surface of the gel layer, where the skin depth is of the order of the wavelength of the perturbation (see Fig. 3 in the text).

i) To the spherically symmetric gel layer, we introduce a xyz-coordinate system so that its xy-coordinate plane is tangent to the outer surface of the gel layer at its origin, $x = y = z = 0$. We define the sign of z-coordinate so that the bulk of the gel is on the side of $z \le 0$. We will consider a small neighborhood of the origin so that the curvature of the gel surface is negligible. This apparently flat gel layer is under lateral tension along the xy-plane.

ii) We introduce a slight sinusoidal perturbation of the surface profile of the gel layer, without allowing the displacement of the gel material. The perturbed surface profile is written as $z = \epsilon_Q \, \mathrm{Re}[e^{iQx+\phi}]$, with the amplitude ϵ_Q, the wave number Q and the phase ϕ being constant.

iii) We then let the gel relax until the mechanical balance is re-established within the layer. By this process the stress components $\sigma_{\alpha\beta}$ with $\alpha = x$, y, or z are also perturbed. We denote by $\delta\sigma_{\alpha\beta}$ the perturbed part of the stress components. These $\delta\sigma_{\alpha\beta}$ obey the following equations:

$$\frac{\partial}{\partial x}\delta\sigma_{x\alpha} + \frac{\partial}{\partial y}\delta\sigma_{y\alpha} + \frac{\partial}{\partial z}\delta\sigma_{z\alpha} = 0,$$

with $\alpha = x$, y, or z We assume that the usual linear elasticity relationship applies to the system. Then the perturbed stress components is related with the displacements (u_x, u_y, u_z) from the unperturbed state through the equation

$$\delta\sigma_{\alpha\beta} = 2\mu\left(u_{\alpha\beta} - \frac{1}{3}\sum_\gamma u_{\gamma\gamma}\delta_{\alpha\beta}\right) + K\sum_\gamma u_{\gamma\gamma}\delta_{\alpha\beta}$$

with

$$u_{\alpha\beta} \equiv \frac{1}{2}\left(\frac{\partial u_\alpha}{\partial x_\beta} + \frac{\partial u_\beta}{\partial x_\alpha}\right),$$

where μ and K are the shear and bulk moduli, the suffices α, β and γ take x, y or z, and $\{x_x, x_y, x_z\} \equiv \{x, y, z\}$. The summation index γ runs over x, y and z, and $\delta_{\alpha\beta}$ is the Kronecker's delta.

iv) The question is how the quantities $\delta\sigma_{\alpha\beta}$ depend on z for $z < 0$. In the lowest order of ϵ_Q, $\delta\sigma_{\alpha\beta}$, and therefore the displacements u_α should depend on x sinusoidally with the wave number, Q. Therefore, the above equations can be reduced to the following matrix equation:

$$\begin{pmatrix} 2\mu\frac{\partial^2}{\partial z^2}-(K+\frac{10}{3}\mu)Q^2 & iQ\frac{\partial}{\partial z} \\ (K+\frac{4}{3}\mu)iQ\frac{\partial}{\partial z} & (K+\frac{10}{3}\mu)\frac{\partial^2}{\partial z^2}-2\mu Q^2 \end{pmatrix}\begin{pmatrix} u_x \\ u_z \end{pmatrix} = \begin{pmatrix} 0 \\ 0 \end{pmatrix}.$$

This equation can be finally reduced to the following equation:

$$(\partial_z{}^2 - Q^2)^2\psi = 0$$

where ψ is a combination of u_x and u_z. From this equation, we find that the displacements should depend exponentially on z. Among mathematically possible forms $e^{\pm Qz}$, we discard the form e^{-Qz} since this factor grows exponentially towards the negative z-axis. We are then left with the form e^{Qz} for $z < 0$. This indicates that the influence of the perturbations to the surface profile with the wavelength $\sim Q^{-1}$ is practically limited within a region with a "skin depth" $\sim Q^{-1}$ from the outer surface of the gel layer.

Appendix D. The derivation of equations (11) and (12)

Here we show how the stress distribution within the gel layer is calculated for the model described by a)-c) in Section 3. In the polar coordinate, the equations of mechanical balance in the gel layer are written as follows:

$$\frac{\partial}{\partial r}(r\sigma_{rr}) + \frac{\partial}{\partial\theta}\sigma_{r\theta} - \sigma_{\theta\theta} = 0,$$

$$\frac{\partial}{\partial r}(r\sigma_{r\theta}) + \frac{\partial}{\partial\theta}\sigma_{\theta\theta} + \sigma_{r\theta} = 0. \tag{D.1}$$

We integrate the left-hand side of these equations with respect to r from r_0 to $r_0 + h$, noting the boundary conditions, equations (10) and (8). The result reads

$$T - \frac{\partial}{\partial \theta} \bar{T} = -r_0 \sigma_{rr}|_{r_0}$$

and

$$\bar{T} + \frac{\partial}{\partial \theta} T = 0,$$

where we have introduced the total tension, $T \equiv \int_{r_0}^{r_0+h} \sigma_{\theta\theta} dr$, and its analogue for the shear stress, $\bar{T} \equiv \int_{r_0}^{r_0+h} \sigma_{r\theta} dr$. Based on our estimates of the shear stress, $\sigma_{r\theta} \sim \tilde{\mu}\epsilon_q (h^*/r_0)^2$, and the perturbed part of the tensile stress, $\delta\sigma_{\theta\theta} \sim \epsilon_q B h^*/r_0$ (see Sect. 3), we can evaluate the terms on the left-hand side of the above equations. Since $\frac{\partial}{\partial \theta} \sim 1$ under our limitation of the wave number q, we have, $\delta T \sim \frac{\partial}{\partial \theta} T \sim B \epsilon_q h^{*2}/r_0$ and $\bar{T} \sim \frac{\partial}{\partial \theta} \bar{T} \sim \tilde{\mu}\epsilon_q h^{*3}/r_0{}^2$, where δT is the perturbed part of the total tension T. Assuming $\tilde{\mu} \sim B$, we find that $\bar{T}$ and $\frac{\partial}{\partial \theta} \bar{T}$ are smaller than T and $\frac{\partial}{\partial \theta} T$ by a factor of h^*/r_0. We, therefore, ignore the terms with $\bar{T}$, and have the following equations:

$$\frac{\partial}{\partial \theta} T = 0, \qquad T = -r_0 \sigma_{rr}|_{r_0}. \qquad (D.2)$$

The first equation requires the lateral balance of the integrated tension T, while the second equation requires the homogeneity of the normal compressive stress on the substrate surface, $\sigma_{rr}|_{r_0}$.

From (D.2) we can calculate $\sigma_{\theta\theta}|_{r_0+h^*}$ and $-\sigma_{rr}|_{r_0}$. We employ the "stacked rubber band model" [5,11,12] for the lateral tensile stress $\sigma_{\theta\theta}$, as we did for the symmetric case (see Eq. (1) in the text). Here, we take into account the possible lateral displacement of the gel layer upon the re-establishment of the mechanical balance. We introduce an unknown function $\theta(\theta_0)$ such that the material of gel layer originally at θ_0 is moved to $\theta(\theta_0)$ upon the re-establishment of the mechanical balance (see Fig. 7). The elongation ratio, $(r - r_0)/r_0$ in equation (1) is, therefore, replaced by the form which depends on the parameter θ_0: $(r d\theta(\theta_0) - r_0 d\theta_0)/r_0 d\theta_0$. Thus, the lateral tension is written as

$$\sigma_{\theta\theta} = B \left(\frac{r}{r_0} \frac{d\theta(\theta_0)}{d\theta_0} - 1 \right), \qquad (D.3)$$

where, the shear deformation within the layer has been consistently ignored. (The justification of this approximation concerning another source of error will be discussed in the discussion section, see App. E.) With the definition of T given above, we obtain

$$T = B \left[\left(h(\theta_0) + \frac{h(\theta_0)^2}{2r_0} \right) \frac{d\theta(\theta_0)}{d\theta_0} - h(\theta_0) \right]. \qquad (D.4)$$

The function $\theta(\theta_0)$ can be related to $h(\theta_0)$ through the first equation in (D.2), which requires that T is constant.
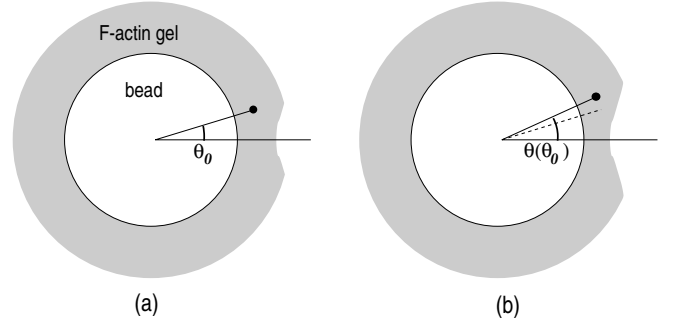

Fig. 7. (a) θ_0 is defined as the angle with respect to a reference line, when a material point (for example, the black dot) is located before the gel is deformed. (b) As a result of elastic deformation, the material point characterized by θ_0 is displaced to a new position at θ. The function $\theta(\theta_0)$ characterizes the elastic deformation.

To fix the value of the constant, T, we recall an apparent condition $\int_0^{2\pi} \frac{d\theta(\theta_0)}{d\theta_0} d\theta_0 = 2\pi$. The result of T is

$$T = B \left[\int_0^{2\pi} \frac{d\theta_0}{h(\theta_0) + \frac{h(\theta_0)^2}{2r_0}} \right]^{-1}$$
$$\times \left[2\pi - \int_0^{2\pi} \frac{h(\theta_0)}{h(\theta_0) + \frac{h(\theta_0)^2}{2r_0}} d\theta_0 \right]. \qquad (D.5)$$

$\frac{d\theta(\theta_0)}{d\theta_0}$ can thus be finally determined in terms of $h(\theta_0)$ (which we do not show explicitly). From the second equation of (D.2) and from equation (D.3), we have

$$\sigma_{\theta\theta}|_{r_0+h(\theta_0)} = \left[h(\theta_0) + \frac{h(\theta_0)^2}{2r_0} \right]^{-1}$$
$$\times \left[T \left(1 + \frac{h(\theta_0)}{r_0} \right) + B \frac{h(\theta_0)^2}{2r_0} \right], \quad (D.6)$$

$$-\sigma_{rr}|_{r_0} = \frac{T}{r_0}. \qquad (D.7)$$

To reach the expressions equations (11) and (12) in the text, we may simply substitute the form $h(\theta_0) = h^* [1 + \epsilon_q \cos(q \theta_0)]$, into equations (D.5-D.6), and develop them with respect to ϵ_q up to the linear order.

Appendix E.

Below we mention briefly aspects which could be improved in our present analysis.

1) *Extend the analysis to modes with $q \neq \frac{2\pi r_0}{h^*}$.*

   Although the instability against the disturbances of modes $q \simeq \frac{2\pi r_0}{h^*}$ is sufficient to destroy the system's stability, our analysis can say nothing about what is the fastest, or the most unstable, mode of the disturbance. The fact that the characteristic time of the symmetry breaking in our analysis gives reasonable values suggests that the other modes of perturbations might

grow, if they do, at a rate not highly exceeding the one we have analyzed. In fact, some efforts to refine the present analysis (see below) indicate that, for $q < \frac{2\pi r_0}{h^*}$, the instability is weakened or even suppressed, while for the modes, $q > \frac{2\pi r_0}{h^*}$, there is no sign of appreciable q-dependences. However, the modulation of the micro-scale comparable to the mesh size of the gel is not accessible by the continuum approach. (Note that the quasi–one-dimensional analysis of [10] claims the instability of the mode $q = 2$.)

2) *Remove the full slip boundary condition.*
   As discussed in Section 3 we have justified this boundary condition when we analyzed the evolution of the modes $q \simeq \frac{2\pi r_0}{h^*}$, since, there, the choice of the boundary condition on the substrate surface is expected to be insensitive to the stability result. For the other modes, especially for $q < \frac{2\pi r_0}{h^*}$, we should take into account the friction on this surface due to the temporal linkage between the actin filament with the substrate [11]. (About the discussion of the relation between the friction and the temporal linkage, see [19,15].) As a modification of the present model, we have incorporated the finite friction force on the substrate surface, which is proportional to the slipping velocity of the gel along the surface. Though details will not be shown [13], the result indicates that, while all the modes remain unstable, the instability is weakened for long wavelengths, *i.e.* for small values of q.

3) *Extend the analysis to the non-linear regime.*
   Our analysis does not infer how the comet of actin gel is formed and continues to grow after the symmetric shape of the layer around the bead is lost. This is a non-linear problem. Van Oudenaarden and Theriot have demonstrated in their numerical modeling that the comet formation shows its optimal performances for a certain parameter value related to the depolymerization at the substrate surface. The comparative study from our point of view is yet to be done. (As for the steady growth of the comet from *Listeria*, see [11]).

4) *Extend the analysis to soft beads.*
   Endosomes, lysosomes, vesicles and fluid drops deform as the comet develops, revealing the importance of mechanical stresses [2,20,21]. The deformation of a fluid drop has been fully analyzed within the framework of the elastic analysis and shown to be quantitatively in agreement with the experiment [22]. The symmetry-breaking onset remains to be worked out. As proposed in the discussion, the early stages would discriminate between the different mechanisms.

5) *Removal of the assumption of the isotropic gel.*
   Generally speaking, the microstructure of the gel polymerized from a surface must distinguish the radial direction from the lateral ones. Especially, the actin gel branched by the help of the protein Arp2/3 is shown to have a topology like a "forest" rather than like a network [23]. It will be the entanglement among the branches of the "trees" of semi-flexible filaments that supports the tensile stress within the gel. Though we expect no qualitative change of our result upon
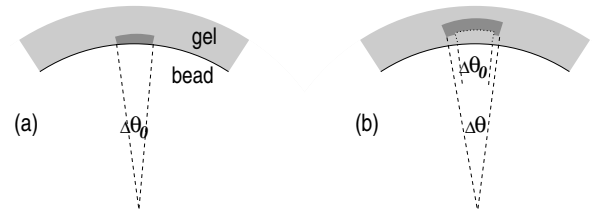

Fig. 8. Generation of a mechanical frustration (internal stress) caused by simultaneous polymerization and lateral deformation; a rectangular piece of gel (marked block) is displaced and deformed while keeping the connectivity with its neighboring piece (block shown by dotted lines).

the incorporation of the elastic anisotropy of the gel, there should be quantitative differences. For the further analysis, we also need the experimental data on the anisotropic elastic constants [12].

6) *Extend the analysis where the gel density is spatially heterogeneous.*
   The effect of the spatial heterogeneity of the catalytic activity of the enzyme may have several aspects. The one which has been discussed in Section 5.2 is the modulation of the polymerization rate, $\bar{k}_p$. The other aspect which is related to the spatial heterogeneity of elastic moduli of gel may also deserve consideration. In fact, the heterogeneity of the elastic moduli will be closely related to the heterogeneity of the factors k_d and c_d both concerning the depolymerization processes kinematically and energetically, respectively. It is therefore impossible to predict where does the thinning of the gel layer proceed most rapidly. However, the rule of thumbs is again that the positive feedback mechanism mentioned above: once the degradation is advanced in a portion of gel layer than elsewhere, the stress concentration is most likely to occur and the degradation will be further accelerated there. Viscoelastic (*e.g.*, of Maxwell or Voigt types) or frictional effects in the bulk gel or on the substrate surface, respectively, may limit this positive feedback loop. A detailed discussion will be the task of future works.

7) *Take account of the frustration of stress in gel.*
   In the analysis of Section 4, the total tension $T \equiv \int_{r_0}^{r_0+h} \sigma_{\theta\theta} \mathrm{d}r$ has been calculated by substituting the expression of the stacked rubber band model, equation (D.3). This operation ignores the fact that the gel material at two different radii are created at different points of time. Figure 8 illustrates how the simultaneous polymerization and lateral deformation create a mechanical frustration within the gel material: (a) Consider a thin slice of actin gel created at the substrate surface during a short time interval, say, between t_1 and $t_1 + \mathrm{d}t$ (the dark gray region occupying the angle $\Delta\theta_0$). We may expect that this part of gel which is just grown bears no lateral stress, to a good approximation. In the context concerning this slice just above the substrate surface, we would then set $\mathrm{d}\theta(\theta_0)/\mathrm{d}\theta_0 = 1$ in equation (D.3). (b) After the consecutive time interval, $t_1 + \mathrm{d}t < t < t_1 + 2\mathrm{d}t$,

the same spatial region, which is now indicated by the dotted lines, is occupied by a newly grown gel under no lateral tension. Thus again $d\theta(\theta_0)/d\theta_0 = 1$ for this region. However, as for the previously grown material which we have marked in dark gray in Figure 8(a), it now occupies the region just outside the original one (shown again in dark gray), and occupies the angle $\Delta\theta$. Generally, $\Delta\theta$ is different from $\Delta\theta_0$ as far as there is a global lateral displacement of gel during the time interval $t_1 + dt < t < t_1 + 2dt$. Thus, in the context concerning this region in dark gray, we would set $d\theta(\theta_0)/d\theta_0 \neq 1$ in equation (D.3). This contradiction indicates a natural process through which a mechanical frustration is created within the gel layer, and shows that equation (D.3) is only approximative.

Taking account of this fact in the model requires a lot of complication of the formalism, but the linear analysis is still feasible. Though the details will not be shown [13], the result indicates that, while the modes with small q values now become stable, the instability persists for $q > q_c$ with a finite positive threshold q_c. Our simple analysis with equation (D.3) is still a good approximation if the characteristic time of the instability τ is short enough as compared with the turnover time of the gel, r_0/v_{gel}. From equation (22) this criterion reads $(2 + \chi)/(c_d B\chi) \ll 1$. Substituting the same values for $c_d = \xi^3/T$, B, and χ as in Section 5.1, the left-hand side of the above criterion becomes 0.16 if we take $\xi = 30$ nm for the mesh size of the actin gel. We, therefore, suppose that our approximation is pretty good for the above parameter range.

References

1. F. Gerbal, V. Laurent, A. Ott, P. Chaikin, J. Prost, Eur. Biophys. J. **29**, 134 (2000).
2. J. Taunton, B.A. Rowning, M.L. Coughlin, M. Wu, R.T. Moon, T.J. Mitchison, C.A. Larabell, J. Cell Biol. **148**, 519 (2000).
3. T.P. Loisel, R. Boujemaa, D. Pantaloni, M.F. Carlier, Nature **401**, 613 (1999).
4. L.A. Cameron, M.J. Footer, A. van Oudenaarden, J.A. Theriot, Proc. Natl. Acad. Sci. U.S.A. **96**, 4908 (1999).
5. V. Noireaux, R.M. Golsteyn, E. Friedrich, J. Prost, C. Antony, D. Louvard, C. Sykes, Biophys. J. **78**, 1643 (2000).
6. D. Yarar, W. To, A. Abo, M.D. Welch, Curr. Biol. **9**, 555 (1999).
7. A. Bernheim-Grosswasser, S. Wiesner, R.M. Goldsteyn, M.-F. Carlier, C. Sykes, Nature **417**, 308 (2002).
8. S. Rafelski, P. Lauer, D. Portnoy, J. Theriot, `http://cmgm.stanford.edu/theriot/movies.htm`: *Skidding motility of mutant Listeria* (2002).
9. A. van Oudenaarden, Julie A. Theriot, Nature Cell Biol. **1**, 493 (1999).
10. A. Mogilner, G. Oster, Biophys. J. **84**, 1591 (2003).
11. F. Gerbal, P. Chaikin, Y. Rabin, J. Prost, Biophys. J. **79**, 2259 (2000).
12. L. Landau, E. Lifchitz, *The Theory of Elasticity* (Mir, Moscow, 1967).
13. K. Sekimoto, F. Jülicher, J. Prost, unpublished (2001).
14. K. Kassner, C. Misbah, J. Muller, J. Kappey, P. Kohlert, Phys. Rev. E **63**, 036117 (2001). (The original literatures on the crystal growth related to the stress concentration, such as R.J. Asaro, W.A. Tiller, Metall. Trans. **3**, 1789 (1972) and M.A. Grinfeld, Dokl. Akad. Nauk USSR **265**, 836 (1982) are cited and described therein.)
15. F. Gerbal, V. Noireaux, C. Sykes, F. Jülicher, P. Chaikin, A. Ott, J. Prost, R.M. Golsteyn, E. Friederich, D. Louvard, V. Laurent, M.F. Carlier, Pramana **53**, 155 (1999).
16. J. Prost, in *Physics of Bio-molecules and Cells, Les Houches Session LXXV, 2-27 July 2001*, edited by H. Flyvbjerg *et al.*, Les Houches Summer School Series, Vol. **75** (Springer, 2002).
17. M. Dogterom, B. Yurke, Science **278**, 856 (1997).
18. J. Plastino, I. Lelidis, J. Prost, C. Sykes, Eur. Biophys. J. (published on line, 09 December, 2003); DOI: 10.1007/s00249-003-0370-3.
19. K. Tawada, K. Sekimoto, J. Theor. Biol. **150**, 193 (1991).
20. P.A. Giardini, D.A. Fletcher, J.A. Theriot, Proc. Natl. Acad. Sci. U.S.A. **100**, 6493 (2003).
21. A. Upadhyaya, J.R. Chabot, A. Andreeva, A. Samadani, A. van Oudenaarden, Proc. Natl. Acad. Sci. U.S.A. **100**, 4521 (2003).
22. O. Campas, J.-F. Joanny, J. Prost, unpublished.
23. L.A. Cameron, T.M. Svitkina, D. Vignjevic, J.A. Theriot, G.G. Borisy, Curr. Biol. **11**, 130 (2001).